Comparison of hemodynamic response functions estimated from resting-state functional MRI and invasive electrophysiological recordings in rats

D Rangaprakash [1,*], Olivier David [2,3], Robert L Barry [1,4], Gopikrishna Deshpande [5,6,7,8]

[1] Athinoula A. Martinos Center for Biomedical Imaging, Massachusetts General Hospital, Harvard Medical School, Charlestown, Massachusetts, USA

[2] Université Grenoble Alpes, F-38000, Grenoble, France

[3] Inserm, U1216, Grenoble Institute of Neuroscience, F-38000, Grenoble, France

[4] Harvard-Massachusetts Institute of Technology Division of Health Sciences & Technology, Cambridge, Massachusetts, USA

[5] AU MRI Research Center, Department of Electrical and Computer Engineering, Auburn University, Auburn, AL, USA

[6] Department of Psychological Sciences, Auburn University, Auburn, AL, USA

[7] Center for Neuroscience, Auburn University, Auburn, AL, USA

[8] Alabama Advanced Imaging Consortium, Birmingham, AL, USA

***Correspondence to:**

D Rangaprakash, Ph.D.

149 13th St, Suite 2.301

Charlestown, MA 02129, USA

Email: RDeshpande3@mgh.harvard.edu

Abstract

Resting-state functional MRI (rs-fMRI) is a popular technology that has enriched our understanding of brain and spinal cord functioning, specifically how different regions communicate (connectivity). But fMRI is an indirect measure of neural activity capturing blood hemodynamics. The hemodynamic response function (HRF) interfaces between the unmeasured neural activity and measured fMRI time series. The HRF is variable across brain regions and individuals, and is modulated by non-neural factors. Ignoring this HRF variability causes errors in FC estimates. Hence, it is crucial to reliably estimate the HRF from rs-fMRI data. Robust techniques have emerged to estimate the HRF from fMRI time series. Although such techniques have been validated non-invasively using simulated and empirical fMRI data, thorough invasive validation using simultaneous electrophysiological recordings, the gold standard, has been elusive. This report addresses this gap in the literature by comparing HRFs derived from invasive intracranial electroencephalogram recordings with HRFs estimated from simultaneously acquired rs-fMRI data in six epileptic rats. We found that the HRF shape parameters (HRF amplitude, latency and width) were significantly similar ($p>0.05$) between ground truth and estimated HRFs. In the single pathological region, the HRF width was marginally significantly different ($p=0.03$). Our study provides preliminary invasive validation for the efficacy of the HRF estimation technique in reliably estimating the HRF non-invasively from rs-fMRI data directly. This has a notable impact on rs-fMRI connectivity studies, and we recommend that HRF deconvolution be performed to minimize HRF variability and improve connectivity estimates.

Keywords: *FMRI; HRF; hemodynamic response; validation; connectivity; resting state*

1. Introduction

Blood oxygenation level-dependent (BOLD) fMRI has been a powerful technology for non-invasively measuring central nervous system (CNS) function [1]. Unlike electroencephalogram (EEG), which directly measures neuronal electrical activity, fMRI only indirectly measures neural activity through local blood oxygenation variations [2] (**Fig.1**). Although oxygen demand is proportional to neural activity, it is also modulated by dilation/constriction of blood vessels that are influenced by several non-neural factors and are thus difficult to delineate [3] (neurovascular coupling). These non-neural factors influence the BOLD signal (variable density/size of vessels, caffeine/alcohol/lipid intake, magnetic susceptibilities, hematocrit, partial volume imaging, respiration/pulse differences [4] [5] [1] [6] [7] [8] [9] [10]). This combination of factors interfacing neural activity to BOLD fMRI is the hemodynamic response function (HRF) [11] [12]. It changes across the brain and individuals [4] [5] [13], since the non-neural factors are variable too.

It has been found that this HRF variability (HRFv) is undesirable in fMRI because it confounds resting-state fMRI (rs-fMRI) connectivity estimates. Specifically, ignoring HRFv results in about 15% error in functional connectivity (FC) estimates in both the brain and spinal cord [14] [15], causing the detection of false positive and false negative connections. Effective connectivity modeling is also viable only after minimizing HRFv [16] [17]. Hence, estimating the HRF and minimizing HRFv is critical to the vast rs-fMRI field.

HRFs estimated from task fMRI data [18] [19] [20] [21] [22] [23] [24] are not directly applicable to rs-fMRI data because a specific task does not activate the entire brain uniformly [25] (HRFs are biased to activated voxels). Even in activated voxels, the BOLD time series could be non-uniform [26], leading to biologically implausible HRF estimates [25]. Further, evidence suggests that spontaneous fluctuations in rs-fMRI can be observed at frequencies not supported by the canonical

HRF [27] [28] [29] [30] [31]. Therefore, it is advisable to directly estimate the HRF from rs-fMRI data to minimize the HRF confound in rs-fMRI connectivity modeling. The HRF cannot be directly measured non-invasively with rs-fMRI, and it may not be possible to estimate HRF latency from a hypercapnic challenge [32] due to the unavailability of a breath-hold fMRI scan or holding breath not being feasible in pathological populations [33].

However, critical technical advancements such as point-process theory [34] [35] have now provided us with deconvolution techniques that can perform HRF estimation with rs-fMRI alone [36] [37] [38] [39]. They have been validated [34] [36] [14] and applied in recent studies [40] [41] [42] [43] [44] [45] [46]. These deconvolution techniques estimate two unknowns (latent neural activity and the HRF) using one input (fMRI time series), which is possible in a least-squares sense because we know the biophysics and natural limits of HRF and fMRI, which constrain the solution space. Although a few excellent rs-fMRI HRF deconvolution techniques are available [47] [37] [38] [39], here we specifically focus on Wu et al.'s method [36]. Extending our results to the other techniques is the scope for future work.

Wu et al.'s method [36] considers rs-fMRI as event-related time series with events modeled as point-processes [48]. It then estimates the least-squares best fit HRF from the fMRI time series at identified events. Latent neural time series is estimated from fMRI and HRF using Wiener deconvolution [49]. This technique is validated non-invasively using simulations and empirical fMRI data [34] [36] [14]; it is well-recognized (~250 citations) and has been utilized in several recent papers (e.g., [14] [40] [41] [42] [43] [44] [45] [46]). However, invasive validation using independent electrophysiological recordings, the gold standard, has been elusive. We addressed this gap by utilizing simultaneous invasive intracranial EEG (iEEG) recordings and rs-fMRI data

acquired in six epileptic rats (thorough data acquisition details are in [50] [51]). We compared the HRFs derived from iEEG with those estimated from fMRI.

2. Results

Three regions of interest (ROIs) were chosen [50], which were the most consistently activated across sessions and animals. They were primary somatosensory cortex barrel field (S1BF), striatum and thalamus. Since S1BF was the pathological region (epileptic focus), an abnormally slow HRF was observed compared to the striatum and thalamus (**Figure 1**). This is understood to be due to the suppression of cerebral blood flow autoregulation mechanisms modulating vasodilatation. Please refer to David et al. [50] for descriptions and other analyses related to the iEEG data used here.

Within a biologically-constrained biophysical model of brain hemodynamics [52] [53], Wiener deconvolution was performed using iEEG (as the neural input) and fMRI [49] to derive the ground truth HRF (replicated from [50], inverted HRFs are rendered as positive). HRF was separately estimated from fMRI also, using Wu et al.'s method [36]. Estimated and ground truth HRFs were compared in all three regions across the six rats [50]. Specifically, we compared the HRF shape parameters (see Figure 1 in [14]) – response height (RH or HRF amplitude), time-to-peak (TTP or HRF latency) and full-width-at-half-max (FWHM or HRF width).

We found an excellent match between the HRFs (**Figure 1**). RH and TTP were not significantly different between estimated and ground truth HRFs in all regions (p>0.05), and FWHM was not different except in S1BF. In S1BF, FWHM was barely significantly different (p=0.03), which would not have been significant if we had performed multiple comparisons correction. The original

study [50] describes S1BF as pathological with abnormal HRF. Despite this, the relative HRF amplitude and timing information were preserved. Overall, except for the FWHM misspecification in a pathological region, the HRF shape estimated from Wu et al.'s technique had significant similarity with the ground truth HRF shape (**Figure 2**).

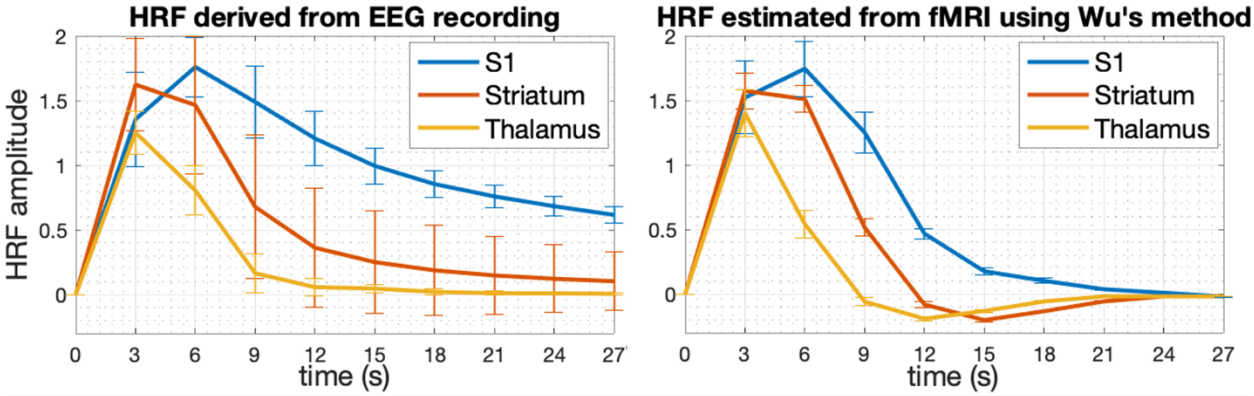

	S1BF			Striatum			Thalamus		
	EEG-HRF	fMRI-HRF	p-value	EEG-HRF	fMRI-HRF	p-value	EEG-HRF	fMRI-HRF	p-value
RH	1.95	1.89	0.82	1.97	1.88	0.61	1.18	1.30	0.36
TTP	11	11	0.91	7.95	7.88	0.92	6	6	0.18
FWHM	27.3	8.6	*0.03*	9	5.3	0.06	5.2	5.1	0.75

Figure 1. *Plots of ground truth iEEG-derived HRF (top-left) vs. Wu et al.'s estimated HRF (top-right). HRF shape parameters were not significantly different between ground truth and estimated HRFs (p>0.05) except for FWHM in one pathological region (p=0.03). The table at the bottom shows median values along with p-values for comparison between ground truth and estimated HRFs (paired t-test was performed for RH, and Wilcoxon sign-rank test was performed for TTP and FWHM). HRF is positive in amplitude; RH is unitless (only relative differences matter); TTP and FWHM are in seconds.*

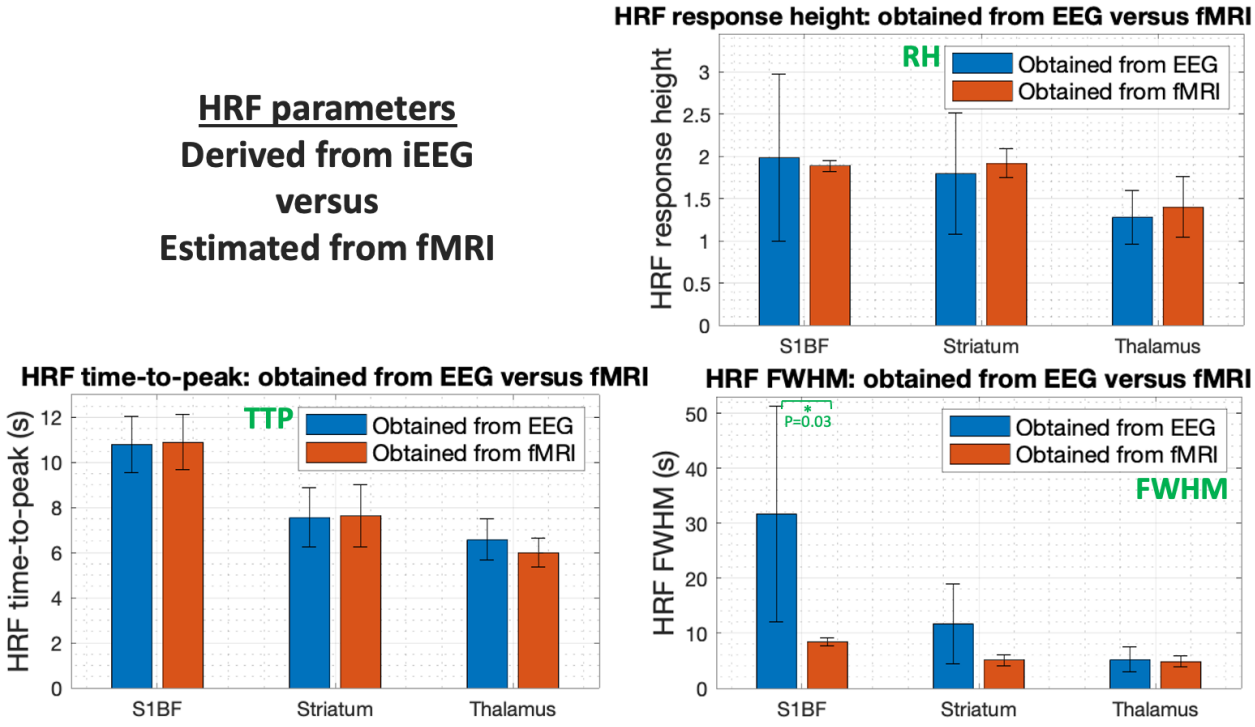

Figure 2. *Bar graphs comparing HRF shape parameters of iEEG-derived ground truth HRF and fMRI-estimated HRF in the three regions of interest. All parameters in all regions were similar except FWHM in the S1BF region, which was different with p=0.03.*

3. Discussion

Our goal was to test whether HRFs estimated non-invasively from rs-fMRI data (without knowledge of the neural input) were similar to HRFs derived invasively using iEEG (with knowledge of the neural input). We tested this in the specific case of six epileptic rats in three ROIs. We found that the two HRFs were similar. The only exception was with one of the shape parameters in one pathological region. Even in this region (S1BF), the HRF amplitude (RH) and timing (TTP) were estimated accurately, but the HRF width (FWHM) was underestimated. Taken together, we concluded that our results provide preliminary invasive validation for Wu et al.'s technique's ability to estimate the HRF from fMRI data in non-pathological regions in rats.

Whether these results extend to humans in both healthy and pathological cases remains to be explored, but it is not straightforward because of the invasive nature of the experimental setup and the necessity for simultaneous iEEG and fMRI acquisition. The impact of fMRI temporal resolution on our results is also unclear because our validation with low temporal resolution data (TR=3s) may or may not extend to higher resolutions (TR<1s) that are not uncommon today. Our results are nevertheless encouraging. The HRF confound is a key issue that is difficult to ignore, and rs-fMRI connectivity is an expanding field of research with dozens of papers published weekly. Given this context, our results are significant because most rs-fMRI studies ignore HRFv and do not perform deconvolution, with one of the reasons being that the HRF estimation techniques lack validation using ground truth obtained from invasive procedures. Our study entrusts a level of confidence in the Wu et al. technique and its ability to estimate the HRF reliably, and provides motivation to conduct further invasive validation studies under various scenarios in humans. Such efforts are also important for other HRF estimation techniques.

The study reported herein is not the first study to attempt invasive validation of Wu et al.'s technique. A recent study from the same group [54] used co-localized intrinsic optical signals (IOS) and local field potentials (LFPs) in a rat to compare the HRF estimated using Wu et al.'s technique from IOS signals with the HRF derived from the envelope of the LFP signal. They found a high correlation between the two HRFs (R=0.82±0.04). However, our study directly used rs-fMRI data instead of IOS signals, which is important because each modality has its stereotypical noise profiles and idiosyncratic processing pipelines that can make a difference to the outcomes. Hence, it is reaffirming that our results validated the Wu et al. method using rs-fMRI data, corroborating what their study validated with IOS signals. Our study also included six rats instead

of one, and three ROIs instead of one. The conclusion from our study supports the conclusions from theirs.

Taken together, our findings support the notion that it is possible to accurately estimate the HRF non-invasively from rs-fMRI data, at least in non-pathological regions in rats. Further research must confirm this in humans under both healthy and pathological cases. We encourage researchers to account for HRFv and minimize the HRF confound in their rs-fMRI connectivity studies. We recommend performing HRF deconvolution and utilizing the estimated latent neural time series in subsequent analyses instead of directly using the BOLD time series.

4. Materials and methods

4.1. Data acquisition

All the data used by us were previously acquired for a different project, and here we performed further processing and secondary analyses to achieve our goals. Complete details of animal preparation, experimental setup, data acquisition and data denoising/preprocessing can be found in [50]. We briefly describe it here for the benefit of the readers.

Data were acquired from Genetic Absence Epilepsy Rats from Strasbourg (GAERS) [55]. These rats exhibited spontaneous spike and wave discharges (SWDs) lasting about 20s and repeating every minute at rest. These epileptic seizures stemmed from an epileptic focus and spread to other brain regions [55]. SWDs originate in perioral regions of S1 (first somatosensory cortex, S1BF) [56] [57]; that is, this region is pathogenic in these rats.

Animal care/experiments were conducted in accordance with the European Community Council Directive of 24 November 1986 (86/609/EEC). They were approved by the animal experimentation Ethical Committee at the Université Joseph Fourier, Grenoble, France (protocol

number 88–06). Six male adult GAERS were included (281±56g). Spontaneous SWDs were measured with iEEG during MRI data acquisition. Three carbon electrodes situated in the skull near the midline were used (frontal, parietal and occipital) for iEEG data acquisition from a digital acquisition system (Cambridge Electronic Design); sampling rate = 2kHz, analog filter passband = 1–90Hz. Two reference electrodes were placed in the occipital and nasal bones. FMRI and iEEG temporal co-registration was done by the iEEG acquisition software using the MRI system's trigger signal during each volume acquisition. MRI data were acquired in a horizontal-bore 2.35 Tesla scanner (Bruker Spectrospin) having actively shielded gradient coils (Magnex Scientific). A linear volume transmit coil and an actively decoupled surface receive coil were used. A gradient-echo echo planar imaging sequence was used for fMRI: two shots, TR/TE = 3000/20ms, flip angle = 90°, voxel size = $0.73\times0.73\times1.5mm^3$, 15 slices, whole brain coverage. Scan duration ranged from 30 to 150 minutes across rats. T1-weighted anatomical data were acquired with a 3D-MDEFT sequence (modified driven equilibrium Fourier transform) [58]: TR/TE = 15/5ms, inversion time = 605ms, flip angle = 22°, voxel size = $0.33\times0.33\times0.33mm^3$.

SPM 5 [59] was used for data processing and quality assurance. Standard spatial preprocessing was performed, including realignment, co-registration and smoothing. Three ROIs were identified [50]: primary somatosensory cortex barrel field (S1BF), thalamus and striatum. Activations were found in S1BF and thalamus, whereas deactivations were found in the striatum [50]. These three regions were selected because (1) they were consistently activated across different sessions and rats; (2) they exhibited a wide range of hemodynamic responses, which is helpful for rigorous validation of our estimated HRFs; and (3) these regions align well with our current understanding of SWDs. Mean time series from these three regions were used in subsequent analysis. Please refer to [50] [51] for complete details of data acquisition and preprocessing.

4.2. Data processing and analyses

All fMRI data processing presented here, as well as the comparison of HRFs, was carried out exclusively for this study. As described before, HRFs were estimated from fMRI time series separately in each ROI of each rat using Wu et al.'s method [36]. It considers rs-fMRI as event-related time series; events are modeled as point-processes (threshold: mean+1SD) [48]. It then estimates the best fit HRF at identified events in the fMRI time series in a least-squares sense. Latent neural time series is then estimated from HRF and fMRI using Wiener deconvolution [49]. A temporal mask with aggregate motion (framewise displacement) <0.3mm is used to avoid false events driven by motion [35]. The HRF shape can be characterized by three parameters (see Figure 1 in [14]) – RH, TTP and FWHM.

The procedure for deriving the HRFs from iEEG is explained in detail in David et al. [50] (the same iEEG-derived HRFs from that study were used here). Briefly, the HRF of each ROI in each rat was obtained using Wiener deconvolution within a biologically-constrained biophysical model of brain hemodynamics [52] [53], with the iEEG time series as the input, fMRI time series as the output and the HRF as the transfer function between the two that was derived. HRF parameters (RH, TTP and FWHM) were then quantified from the derived HRFs.

We statistically compared the HRF shape parameters estimated from fMRI with the corresponding iEEG-derived HRF parameters. A paired t-test was performed for RH (continuous variable), and a Wilcoxon sign-rank test was performed for TTP and FWHM (discrete variables, with the smallest unit being one sample or TR).

CRediT (Contributor Roles Taxonomy) – author contributions

D Rangaprakash: Conceptualization, Methodology, Data Analysis, Investigation, Visualization, Writing - Original Draft, Reviewing and Editing. **Olivier David**: Data Acquisition, Investigation, Writing - Reviewing and Editing. **Robert L Barry**: Funding Acquisition, Project Administration, Investigation, Writing - Reviewing and Editing, Supervision. **Gopikrishna Deshpande**: Funding Acquisition, Project Administration, Conceptualization, Methodology, Investigation, Writing - Reviewing and Editing, Supervision.

Disclosures

The authors report no competing interests related to the contents of this manuscript.

Acknowledgments

Secondary data analyses were supported in part by the National Institutes of Health (NIH) through grants R01EB027779 and R21EB031211 (R.L.B.). The content is solely the responsibility of the authors and does not necessarily represent the official views of the NIH.

References

[1] R. B. Buxton, "Introduction to Functional Magnetic Resonance Imaging: Principles and Techniques," *Energy,* vol. 24, no. 2, pp. xi, 523, 2002.

[2] N. K. Logothetis, J. Pauls, M. Augath, T. Trinath and A. Oeltermann, "Neurophysiological investigation of the basis of the fMRI signal," *Nature,* vol. 412, pp. 150-157, 2001.

[3] F. Biessmann, Y. Murayama, N. Logothetis, K. Müller and F. Meinecke, "Improved decoding of neural activity from fMRI signals using non-separable spatiotemporal deconvolutions," *Neuroimage,* vol. 61, no. 4, pp. 1031-42, 2012.

[4] D. A. Handwerker, J. M. Ollinger and M. D'Esposito, "Variation of BOLD hemodynamic responses across subjects and brain regions and their effects on statistical analyses," *Neuroimage,* vol. 21, no. 4, pp. 1639-51, 2004.

[5] G. K. Aguirre, E. Zarahn and M. D'esposito, "The variability of human, BOLD hemodynamic responses," *Neuroimage,* vol. 8, no. 4, pp. 360-9, 1998.

[6] J. M. Levin, M. H. Ross, J. H. Mendelson, M. J. Kaufman, N. Lange, L. C. Maas, N. K. Mello, B. M. Cohen and P. F. Renshaw, "Reduction in BOLD fMRI response to primary visual stimulation following alcohol ingestion," *Psychiatry Research,* vol. 82, no. 3, p. 135–46, 1998.

[7] M. D. Noseworthy, J. Alfonsi and S. Bells, "Attenuation of brain BOLD response following lipid ingestion," *Human Brain Mapping,* vol. 20, no. 2, p. 116–121, 2003.

[8] H. S. Yang, Z. Liang, J. F. Yao, X. Shen, B. D. Frederick and Y. Tong, "Vascular effects of caffeine found in BOLD fMRI.," *Journal of neuroscience research,* vol. 97, no. 4, p. 456–466, 2019.

[9] Y. Tong and B. D. Frederick, "Tracking cerebral blood flow in BOLD fMRI using recursively generated regressors," *Human brain mapping,* vol. 35, no. 11, p. 5471–5485, 2014.

[10] M. Bernier, S. C. Cunnane and K. Whittingstall, "The morphology of the human cerebrovascular system.," *Human brain mapping,* vol. 39, no. 12, p. 4962–4975, 2018.

[11] J. H. Kim and D. Ress, "Arterial impulse model for the BOLD response to brief neural activation," *Neuroimage,* vol. 124(Pt A), pp. 394-408, 2016.

[12] J. V. Duarte, J. M. Pereira, B. Quendera, M. Raimundo, C. Moreno, L. Gomes, F. Carrilho and M. Castelo-Branco, "Early disrupted neurovascular coupling and changed event level hemodynamic response function in type 2 diabetes: an fMRI study," *Journal of Cerebral Blood Flow and Metabolism,* vol. 35, no. 10, pp. 1671-1680, 2015.

[13] L. D. Lewis, K. Setsompop, B. R. Rosen and J. R. Polimeni, "Stimulus-dependent hemodynamic response timing across the human subcortical-cortical visual pathway identified through high spatiotemporal resolution 7T fMRI.," *NeuroImage,* vol. 181, p. 279–291, 2018.

[14] D. Rangaprakash, G.-R. Wu, D. Marinazzo, X. Hu and G. Deshpande, "Hemodynamic response function (HRF) variability confounds resting-state fMRI functional connectivity," *Magnetic Resonance in Medicine,* vol. 80, no. 4, pp. 1697-1713, 2018.

[15] D. Rangaprakash and R. L. Barry, "Variability of the hemodynamic response function in the healthy human cervical spinal cord at 3 Tesla," in *International Society for Magnetic Resonance in Medicine annual meeting*, (virtual), 2021.

[16] G. Deshpande and X. Hu, "Investigating effective brain connectivity from fMRI data: past findings and current issues with reference to Granger causality analysis," *Brain Connectivity,* vol. 2, no. 5, pp. 235-45, 2012.

[17] G. Deshpande, K. Sathian and X. Hu, "Effect of hemodynamic variability on Granger causality analysis of fMRI," *Neuroimage,* vol. 52, no. 3, pp. 884-96, 2010.

[18] D. R. Gitelman, W. D. Penny, J. Ashburner and K. J. Friston, "Modeling regional and psychophysiologic interactions in fMRI: the importance of hemodynamic deconvolution.," *NeuroImage,* vol. 19, no. 1, p. 200–207, 2003.

[19] I. Khalidov, J. Fadili, F. Lazeyras, D. Van De Ville and M. Unser, "Activelets: Wavelets for sparse representation of hemodynamic responses," *Signal Processing,* vol. 91, no. 12, pp. 2810-2821, 2011.

[20] C. C. Gaudes, N. Petridou, I. L. Dryden, L. Bai, S. T. Francis and P. A. Gowland, "Detection and characterization of single-trial fMRI bold responses: paradigm free mapping.," *Human brain mapping,* vol. 32, no. 9, p. 1400–1418, 2011.

[21] C. Caballero Gaudes, N. Petridou, S. T. Francis, I. L. Dryden and P. A. Gowland, "Paradigm free mapping with sparse regression automatically detects single-trial functional magnetic resonance imaging blood oxygenation level dependent responses.," *Human brain mapping,* vol. 34, no. 3, p. 501–518, 2013.

[22] L. Hernandez-Garcia and M. O. Ulfarsson, "Neuronal event detection in fMRI time series using iterative deconvolution techniques.," *Magnetic resonance imaging,* vol. 29, no. 3, p. 353–364, 2011.

[23] K. Bush and J. Cisler, "Decoding neural events from fMRI BOLD signal: a comparison of existing approaches and development of a new algorithm.," *Magnetic resonance imaging,* vol. 31, no. 6, p. 976–989, 2013.

[24] K. Bush, J. Cisler, J. Bian, G. Hazaroglu, O. Hazaroglu and C. Kilts, "Improving the precision of fMRI BOLD signal deconvolution with implications for connectivity analysis.," *Magnetic resonance imaging,* vol. 33, no. 10, p. 1314–1323, 2015.

[25] A. J. Taylor, J. H. Kim and D. Ress, "Characterization of the hemodynamic response function across the majority of human cerebral cortex," *Neuroimage,* vol. 173, pp. 322-331, 2018.

[26] J. Gonzalez-Castillo, Z. Saad, D. Handwerker, S. Inati, N. Brenowitz and P. Bandettini, "Whole-brain, time-locked activation with simple tasks revealed using massive averaging and model-free analysis," *Proc Natl Acad Sci USA,* vol. 109, no. 14, pp. 5487-92, 2012.

[27] J. Chen and G. Glover, "Evidence of faster hemodynamic response function at weak sensory stimulus levels supports higher frequency intrinsic functional connectivity.," in *International Society for Magnetic Resonance in Medicine (ISMRM) Annual Meeting*, Paris, France, 2018.

[28] J. E. Chen, G. H. Glover, N. E. Fultz, B. R. Rosen, J. R. Polimeni and L. D. Lewis, "Investigating mechanisms of fast BOLD responses: The effects of stimulus intensity and of spatial heterogeneity of hemodynamics.," *NeuroImage,* vol. 245, p. 118658, 2021.

[29] S. R. Gohel and B. B. Biswal, "Functional integration between brain regions at rest occurs in multiple-frequency bands.," *Brain connectivity,* vol. 5, no. 1, p. 23–34, 2015.

[30] J. E. Chen and G. H. Glover, "BOLD fractional contribution to resting-state functional connectivity above 0.1 Hz.," *NeuroImage,* vol. 107, p. 207–218, 2015.

[31] H. L. Lee, B. Zahneisen, T. Hugger, P. LeVan and J. Hennig, "Tracking dynamic resting-state networks at higher frequencies using MR-encephalography.," *NeuroImage,* vol. 65, p. 216–222, 2013.

[32] C. Chang, M. E. Thomason and G. H. Glover, "Mapping and correction of vascular hemodynamic latency in the BOLD signal.," *NeuroImage,* vol. 43, no. 1, p. 90–102, 2008.

[33] V. R. Spano, D. M. Mandell, J. Poublanc, K. Sam, A. Battisti-Charbonney, O. Pucci, J. S. Han, A. P. Crawley, J. A. Fisher and D. J. Mikulis, "CO2 blood oxygen level-dependent MR mapping of cerebrovascular reserve in a clinical population: safety, tolerability, and technical feasibility.," *Radiology,* vol. 266, no. 2, p. 592–598, 2013.

[34] E. Tagliazucchi, P. Balenzuela, D. Fraiman and D. R. Chialvo, "Criticality in large-scale brain fMRI dynamics unveiled by a novel point process analysis," *Frontiers in Physiology,* vol. 3, p. 15, 2012.

[35] J. D. Power, B. L. Schlaggar and S. E. Petersen, "Recent progress and outstanding issues in motion correction in resting state fMRI," *Neuroimage,* vol. 105, pp. 536-51, 2015.

[36] G. R. Wu, W. Liao, S. Stramaglia, J. R. Ding, H. Chen and D. Marinazzo, "A blind deconvolution approach to recover effective connectivity brain networks from resting state fMRI data," *Medical Image Analysis,* vol. 17, no. 3, pp. 365-374, 2013.

[37] M. Havlicek, K. J. Friston, J. Jan, M. Brazdil and V. D. Calhoun, "Dynamic modeling of neuronal responses in fMRI using cubature Kalman filtering," *Neuroimage,* vol. 56, no. 4, pp. 2109-28, 2011.

[38] M. Havlicek, A. Roebroeck, K. Friston, A. Gardumi, D. Ivanov and K. Uludag, "Physiologically informed dynamic causal modeling of fMRI data.," *NeuroImage,* vol. 122, p. 355–372, 2015.

[39] F. I. Karahanoğlu, C. Caballero-Gaudes, F. Lazeyras and D. Van de Ville, "Total activation: fMRI deconvolution through spatio-temporal regularization.," *NeuroImage,* vol. 73, p. 121–134, 2013.

[40] D. Rangaprakash, G. Deshpande, T. A. Daniel, A. M. Goodman, J. L. Robinson, N. Salibi, J. S. Katz, T. S. Denney and M. N. Dretsch, "Compromised Hippocampus-Striatum Pathway as a Potential Imaging Biomarker of Mild Traumatic Brain Injury and Posttraumatic Stress Disorder," *Human Brain Mapping,* vol. 38, no. 6, pp. 2843-2864, 2017.

[41] D. Rangaprakash, M. N. Dretsch, W. Yan, J. S. Katz, T. S. Denney and G. Deshpande, "Hemodynamic variability in soldiers with trauma: Implications for functional MRI connectivity studies," *NeuroImage: Clinical,* vol. 16, pp. 409-417, 2017.

[42] M. Boly, S. Sasai, O. Gosseries, M. Oizumi, A. Casali, M. Massimini and G. Tononi, "Stimulus set meaningfulness and neurophysiological differentiation: a functional magnetic resonance imaging study," *PLoS One,* vol. 10, no. 5, p. e0125337, 2015.

[43] D. Rangaprakash, M. N. Dretsch, W. Yan, J. S. Katz, T. S. Denney and G. Deshpande, "Hemodynamic response function parameters obtained from resting-state functional MRI data in soldiers with trauma," *Data in Brief,* vol. 14, pp. 558-562, 2017.

[44] E. Amico, F. Gomez, C. Di Perri, A. Vanhaudenhuyse, D. Lesenfants, P. Boveroux, V. Bonhomme, J. F. Brichant, D. Marinazzo and S. Laureys, "Posterior cingulate cortex-related co-activation patterns: a resting state FMRI study in propofol-induced loss of consciousness," *PLoS One,* vol. 9, no. 6, p. e100012, 2014.

[45] B. Lamichhane, B. M. Adhikari, S. F. Brosnan and M. Dhamala, "The neural basis of perceived unfairness in economic exchanges," *Brain Connectivity,* vol. 4, no. 8, pp. 619-30, 2014.

[46] D. Rangaprakash, M. N. Dretsch, A. Venkatraman, J. S. Katz, T. S. Denney and G. Deshpande, "Identifying Disease Foci from Static and Dynamic Effective Connectivity Networks: Illustration in Soldiers with Trauma," *Human Brain Mapping,* vol. 39, no. 1, pp. 264-287, 2018.

[47] K. J. Friston, J. Kahan, B. Biswal and A. Razi, "A DCM for resting state fMRI," *NeuroImage,* vol. 94, no. 100, p. 396-407, 2014.

[48] Z. S. Saad, S. J. Gotts, K. Murphy, G. Chen, H. J. Jo, A. Martin and R. W. Cox, "Trouble at rest: how correlation patterns and group differences become distorted after global signal regression," *Brain Connectivity,* vol. 2, no. 1, pp. 25-32, 2012.

[49] G. H. Glover, "Deconvolution of impulse response in event-related BOLD fMRI," *Neuroimage,* vol. 9, no. 4, pp. 416-29, 1999.

[50] O. David, I. Guillemain, S. Saillet, S. Reyt, S. Deransart, C. Segebarth and A. Depaulis, "Identifying neural drivers with functional MRI: an electrophysiological validation," *PLoS Biology,* vol. 23, no. 6, pp. 2683-97, 2008.

[51] Y. Wang, O. David, X. Hu and G. Deshpande, "Can Patel's τ accurately estimate directionality of connections in brain networks from fMRI?," *Magn Reson Med.,* vol. 78, no. 5, p. 2003-2010, 2017.

[52] K. J. Friston, L. Harrison and W. Penny, "Dynamic causal modelling," *NeuroImage,* vol. 19, no. 4, p. 1273–1302, 2003.

[53] K. J. Friston, A. Mechelli, R. Turner and C. J. Price, "Nonlinear responses in fMRI: the Balloon model, Volterra kernels, and other hemodynamics," *NeuroImage,* vol. 12, no. 4, p. 466–477, 2000.

[54] G. R. Wu, N. Colenbier, S. Van Den Bossche, K. Clauw, A. Johri, M. Tandon and D. Marinazzo, "rsHRF: A toolbox for resting-state HRF estimation and deconvolution.," *NeuroImage,* vol. 244, p. 118591, 2021.

[55] L. Danober, C. Deransart, A. Depaulis, M. Vergnes and C. Marescaux, "Pathophysiological mechanisms of genetic absence epilepsy in the rat.," *Progress in neurobiology,* vol. 55, no. 1, p. 27–57, 1998.

[56] P. O. Polack, I. Guillemain, E. Hu, C. Deransart, A. Depaulis and S. Charpier, "Deep layer somatosensory cortical neurons initiate spike-and-wave discharges in a genetic model of absence seizures.," *The Journal of neuroscience,* vol. 27, no. 24, p. 6590–6599, 2007.

[57] H. K. Meeren, J. P. Pijn, E. L. Van Luijtelaar, A. M. Coenen and F. H. Lopes da Silva, "Cortical focus drives widespread corticothalamic networks during spontaneous absence seizures in rats.," *The Journal of neuroscience,* vol. 22, no. 4, p. 1480–1495, 2002.

[58] R. Deichmann, C. Schwarzbauer and R. Turner, "Optimisation of the 3D MDEFT sequence for anatomical brain imaging: technical implications at 1.5 and 3 T.," *NeuroImage,* vol. 21, no. 2, p. 757–767, 2004.

[59] K. J. Friston, J. Ashburner, S. J. Kiebel, T. E. Nichols and W. D. Penny, Statistical Parametric Mapping: The Analysis of Functional Brain Images, Academic Press, 2007.